Displacement-based Analysis and Design of Rocking Structures

17th World Conference on Earthquake Engineering, 17WCEE
Sendai, Japan - September 13th to 18th 2020
Paper N° C003725
Registration Code: S- A01266

DISPLACEMENT-BASED ANALYSIS AND DESIGN OF ROCKING STRUCTURES

M. F. Vassiliou [1], N. Reggiani Manzo [2]

[1] Assistant Professor, Chair of Seismic Design and Analysis, IBK, ETH Zurich, vassiliou@ibk.baug.ethz.ch
[2] PhD Candidate, Chair of Seismic Design and Analysis, IBK, ETH Zurich, reggianimanzo@ibk.baug.ethz.ch

Abstract

Rocking can be used as a seismic isolation strategy for bridges and buildings. Letting a structure uplift works as a mechanical fuse and limits the design forces of both the foundation and the superstructure. Interestingly, there is no correlation between the rocking oscillator and the elastic one. Therefore, there is not any "equivalent linear system" and the elastic spectra are useless when it comes to rocking. Thus, there is no simplified design procedure that a practicing engineer could use. In order to create design rocking spectra, the rocking oscillator should be described with the simplest possible way and the least necessary parameters. Since Housner's seminal paper in 1963 the traditional DOF chosen to describe the motion of a rocking block has been its tilt angle. This description uncovers that out of two blocks with the same slenderness ratio, the larger one is more stable. This tilt-based description is mathematically correct, but not optimal.

This paper shows that the top displacement is a better descriptor of the rocking oscillator, because it uncovers a fundamental property useful for design: As long as the blocks are not close to overturning, the top displacements of a large and a small block of the same slenderness are going to be roughly equal. This property is proven for both analytical pulses and for recorded ground motions. In mathematical terms, the displacement *demand* on a rocking block is a unary function of its slenderness angle. In practical terms, this means that the displacement demand of any block can be computed by the displacement of a block of the same slenderness, yet very large size – likewise the displacement demand of a yielding oscillator can be computed based on the displacement of an equivalent linear system. Thus, the rocking-related seismic hazard can be computed by much simpler rocking spectra.

As an example, the proposed method is applied for the preliminary design of a rocking frame having the dimensions of a typical overpass bridge.

Keywords: rocking; uplifting structures; dimensional analysis; dimensionality reduction; displacement-based design

1. Introduction

The systematic study of the rocking oscillator started with Housner's seminal paper in 1963 [1]. Since then, it has attracted the interest of many researchers either studying it from a theoretical perspective [2-12] or focusing on using rocking as a seismic isolation technique for bridges [13-24] or buildings [25-28], and on understanding the response of equipment [29-35], ancient temples [36-39], and of masonry walls [40-46].

Unlike the archetype elastic oscillator, which is traditionally described in terms of displacements, the rocking one is usually described in terms of rotations. This emerges naturally as it facilitates the algebraic manipulations to derive the equation of motion. This approach is, of course, mathematically correct. This paper suggests that using displacements instead of rotations to describe the rocking block is physically more meaningful and it simplifies the problem because it reduces its dimension.

2. Rotation based dimensional analysis of the rocking oscillator

The equation of in-plane motion for a rigid rectangular rocking column with slenderness α and a semi-diagonal of length R (Fig. 1) is:

$$\ddot{\theta} = -p^2 \cdot \left(\sin\left[\pm\alpha - \theta\right] + \frac{\ddot{u}_g}{g} \cos\left[\pm\alpha - \theta\right] \right) \tag{1}$$

where

$$p = \sqrt{(3g)/(4R)} \tag{2}$$

is the frequency parameter of the rocking column. The upper sign in front of α corresponds to a positive, and the lower to a negative rocking angle θ with respect to the defined coordinate system (Fig. 1).

It is assumed that energy is only dissipated during impact. Under Housner's assumptions [1] the ratio of post to pre impact rotational velocities is

$$r = 1 - \frac{3}{2}\sin^2\alpha \tag{3}$$

By inspecting Eq. (1) and (2) one can conclude that the rotational response of a rocking block to a ground motion is a function of

$$\theta_{\max} = f_1\left(R, \alpha, g, \ddot{u}_g(t)\right) \tag{4}$$

As the gravity acceleration, g, is constant, the rotational response to a given ground motion is a function of 2 parameters α and R, likewise for the elastic oscillator the response is a function of the eigenperiod, T, and damping ratio ζ. Therefore, keeping one parameter constant (R or α) one can construct rotational spectra for rocking structures. However, unlike the elastic oscillator, where for ordinary structures one parameter (T) is more influential than the other (ζ), in the case of rocking structures, both R and α strongly influence the rotational response.

Since ground motions containing distinguishable acceleration and/or velocity pulses are particularly destructive, Zhang and Makris [47] have studied the response of a planar rocking block to acceleration pulses given by analytical expressions. A pulse of a given waveform can be described by two parameters. Zhang and Makris [47] chose the acceleration amplitude a_p and the dominant cyclic frequency ω_p. Then, the response will be a function of

$$\theta_{\max} = f_2\left(R, \alpha, g, a_p, \omega_p\right) \tag{5}$$

Eq. (5) involves 6 quantities with 2 reference dimensions (Time and Length). Therefore, according to Buckingham's Π-Theorem of Dimensional Analysis [48], the number of dimensionless parameters describing the problem is 6 – 2 = 4. There is not a unique solution on how these four parameters can be chosen. Zhang and Makris [47] and subsequently Dimitrakopoulos and DeJong [49] suggested to describe the problem as

$$\theta_{\max} = \varphi_1\left(\alpha, \frac{\omega_p}{p}, \frac{a_p}{g\tan\alpha}\right) \tag{6}$$

Therefore, dimensional analysis has succeeded to reduce the dimensionality of the problem from 6 to 4. Hence, by keeping the slenderness parameter α constant, one can produce contour plots of the maximum tilt angle θ as a function of ω_p/p and $a_p/g\tan\alpha$, the so called "rocking spectra". Fig. 2 shows the rocking spectra of symmetric and antisymmetric Ricker wavelets. Ricker wavelets are defined as the 2nd and 3rd derivative of the Gaussian [50].

The spectra confirm the remarkable observation that larger structures are harder to overturn dynamically and that higher frequency pulses have a lower overturning potential. Interestingly, they show a heavy dependence of the response to both ω_p/p and $a_p/g\tan\alpha$.

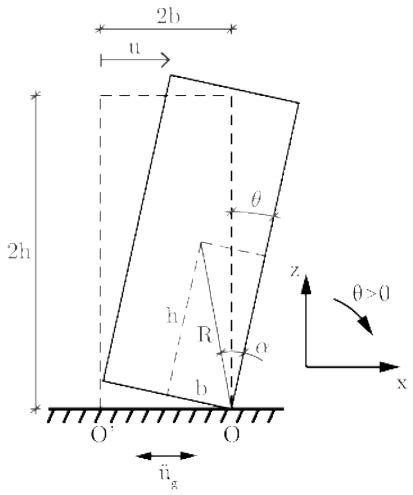

Fig. 1 – Geometric characteristics of the rigid rocking block

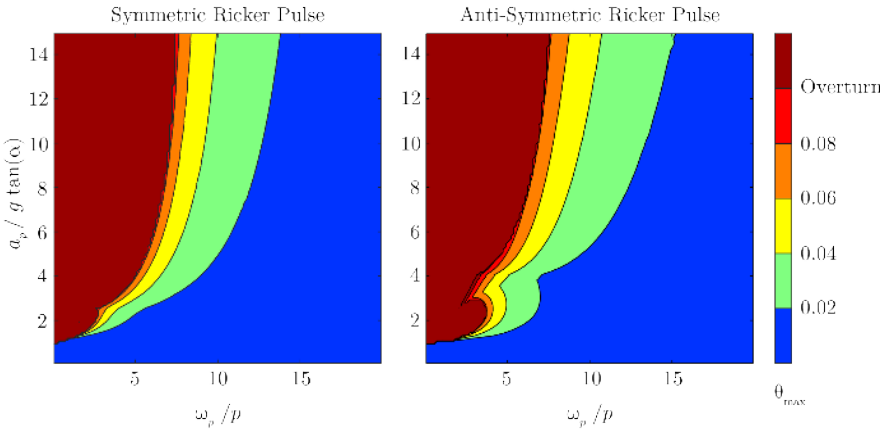

Fig. 2 – Non-dimensional rocking spectra based on rotations. $\alpha = 0.1$

3. Displacement based dimensional analysis of the rocking oscillator

The dimensional analysis in the previous section is one of the many correct solutions to describe the problem. It is based on rotations. This section suggests that there is an alternative, displacement based basis of describing the problem, which is also mathematically correct and more convenient. The convenience does not lie only in the fact that earthquake engineers are more used to displacements than rotations: A displacement based analysis further reduces the dimensionality of the problem allowing the construction of 2D overturning spectra.

Indeed, the rotation based analysis of the problem is based on the "recipe for similarity analysis" described in Chapter 5 of the well-known Dimensional Analysis textbook of G. I. Barenblatt [51]: "*If the problem has an explicit mathematical formulation, the independent variables in the problem and the constant parameters that appear in the equations, boundary conditions and initial conditions, etc., are adopted as the governing parameters.*" However, as this section shows, choosing the parameters that appear in the analytical equation might not be the most convenient way of describing this particular problem.

The top displacement of the rocking block can be obtained by a one-to-one mapping of the rotations:

$$u = 2R\sin\left(\pm\alpha\right) - 2R\sin\left(\pm\alpha - \theta\right) \tag{7}$$

The upper sign in front of α corresponds to a positive, and the lower sign to a negative tilt angle θ with respect to the defined coordinate system.

If we use the top displacement as the single DOF of the problem, then the maximum response can be described as:

$$u_{\max} = f_3\left(R, \alpha, g, a_p, \omega_p\right) \tag{8}$$

To numerically compute the response of the block, we will resort to Eq. (1), which is given in terms of rotation θ. Then, using Eq. (7) we compute the displacement response.

Applying Buckingham's Π-theorem on Eq. (8), one possible non-dimensionalization is

$$\frac{u_{\max}\omega_p^{\,2}}{a_p} = \varphi_2\left(\alpha, \frac{\omega_p}{p}, \frac{a_p}{g\tan\alpha}\right) \tag{9}$$

Fig. 3 shows the contour plots of $\frac{u_{\max}\omega_p^{\,2}}{a_p}$ as a function of $\frac{\omega_p}{p}$ and $\frac{a_p}{g\tan\alpha}$ for a given $\alpha = 0.1$. The remarkable observation is that within the non-overturning region the non-dimensional displacement depends heavily on the non-dimensional strength $\frac{a_p}{g\tan\alpha}$, but only loosely on the size-frequency parameter $\frac{\omega_p}{p}$. When the block is not close to overturning, the influence of $\frac{\omega_p}{p}$ is practically negligible.

Fig. 4 plots $\frac{u_{\max}\omega_p^2}{a_p}$ as a function of $\frac{a_p}{g\tan\alpha}$ for different values of $\frac{\omega_p}{p}$ (and a constant slenderness α = *0.1*). Fig. 5 plots $\frac{u_{\max}\omega_p^2}{a_p}$ as a function of $\frac{\omega_p}{p}$ for different values of $\frac{a_p}{g\tan\alpha}$ (and slenderness α = *0.1*). Again, it is observed that the dominant factor that influences $\frac{u_{\max}\omega_p^2}{a_p}$ is $\frac{a_p}{g\tan\alpha}$; not $\frac{\omega_p}{p}$.

In other words, a small and a large block, geometrically similar to each other, will have roughly equal top displacement, provided that the displacement is not enough to bring them close to overturn. A given earthquake will induce the same *displacement demand*. The larger block is more stable simply because its displacement capacity (i.e. the displacement needed to cause overturn, i.e. its width) is larger.

Therefore, using a displacement basis to describe the problem further decreases the number of parameters needed to define it. Practically, the displacement demand on a rocking oscillator is only a function of its non-dimensional strength $\frac{a_p}{g\tan\alpha}$; not of its size.

Going back to dimensional quantities, Fig. 6 plots the displacement response to a symmetric Ricker pulse with a_p = 1g and T_p = 0.5s and to an antisymmetric Ricker pulse with a_p = 1g and T_p = 1s. The plots confirm that the displacement demand only loosely depends on the size. The dominant factor is the slenderness. Therefore we can define the displacement demand rocking spectrum of a ground motion as a unary function

$$u_{demand} = f(\alpha) \tag{10}$$

that is computed via Eq. (1) and (7) for a large enough block size. To check the stability of a block, one has to compute the maximum displacement demand via Eq. (10) and compare it with the displacement capacity (i.e. the block width).

Therefore, the reduction of the dimension of the problem follows two steps: a) Applying Buckingham's theorem and b) Observing that the displacement demand is roughly independent of the size. The first step is exact and follows from dimensional analysis. The second step is approximate and in this section illustrated for analytical pulses. Blöchlinger [52] gives a first indication, that the approximation also works for recorded ground motions. Further evidence supporting this approximation and highlighting its limitations are given in a next section of this paper.

4. Displacement based analysis of a rocking oscillator excited by recorded ground motions

Analytical pulses can be used to qualitatively study the rocking oscillator. However, as the rocking problem is very sensitive to all of its parameters, pulses would not suffice to prove that the displacement demand on a rocking structure depends only on its slenderness and not on its size. Therefore, this section examines the displacement response of a rocking block excited by recorded ground motions.

4.1 FEMA P695 Ground motions

There is no consensus in the engineering community on what ground motions should be used in time history analysis. Several approaches exist including using recorded (scaled or unscaled), artificial, or synthetic ground motions. In this paper we choose to use the 3 sets of ground motions proposed by FEMA P695 [53] (far field, near field pulse-like, and near field non-pulse-like) only as a means to illustrate our rocking-related argument, without taking stance on the debate around ground motions. It is evident that any ground motion

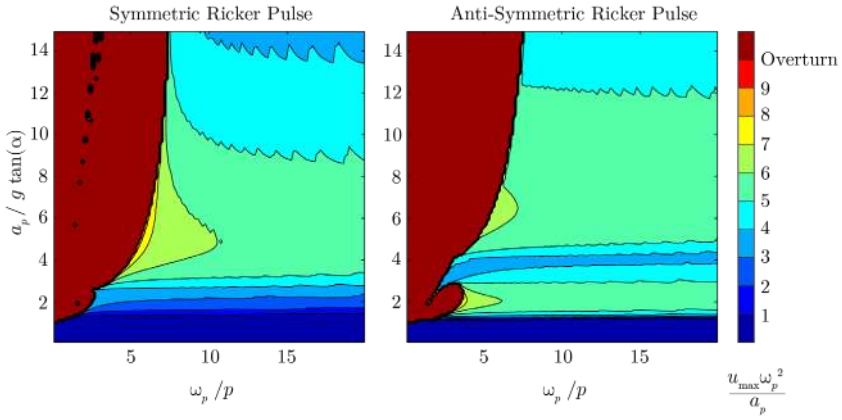

Fig. 3 – Displacement based non-dimensional rocking spectra. $\alpha = 0.1$

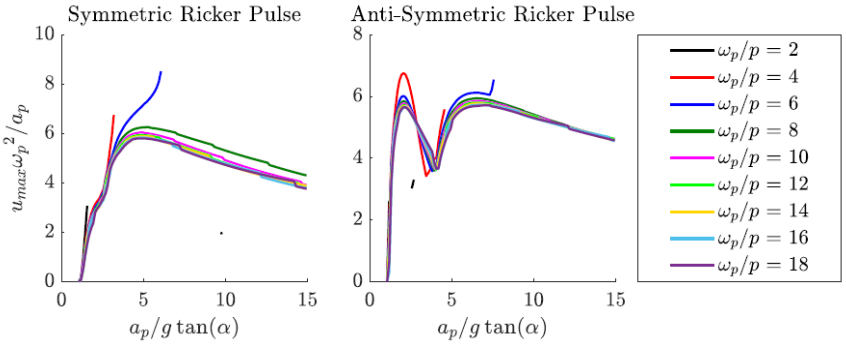

Fig. 4 – $^{u_{max}\omega_p^2}/_{a_p}$ vs $^{a_p}/_{g\tan\alpha}$ plots for constant $^{\omega_p}/_{p}$. $\alpha = 0.1$.

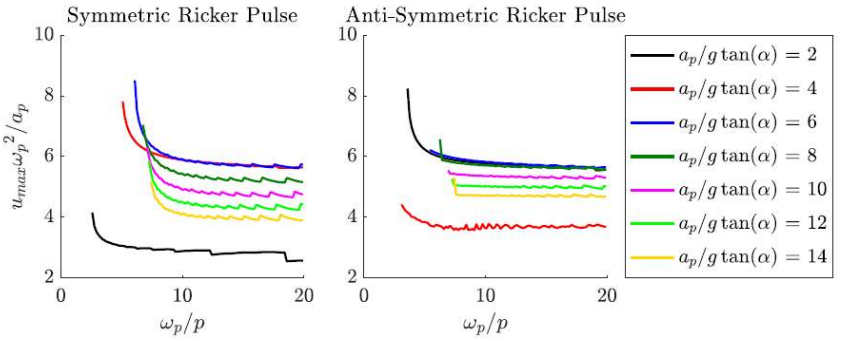

Fig. 5 – $^{u_{max}\omega_p^2}/_{a_p}$ vs $^{\omega_p}/_{p}$ plots for constant $^{a_p}/_{g\tan\alpha}$. $\alpha = 0.1$.

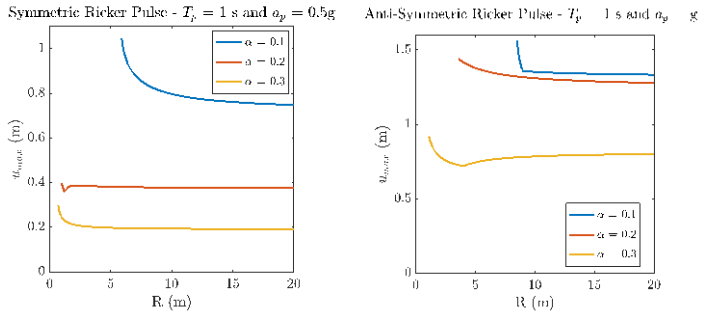

Fig. 6 – Maximum displacement vs block size for Symmetric and Anti-Symmetric Ricker excitation.

selection method based on the response of an elastic system is in principle not applicable in the case of the rocking oscillator, as the elastic and rocking oscillator are uncorrelated. More information on the FEMA P695 ground motions can be found in FEMA [53].

4.2 Equal displacement rule for rocking structures and displacement demand spectra

Vassiliou et al. [54] have proven that rigid rocking oscillators of equal height attached to massless foundations of the same size behave identically, no matter what their actual column width is (Fig. 7). Therefore, the design question of a rocking structure would be: Find the size, *2B'*, of the foundation for a given oscillator height 2*H*. Hence, it is more meaningful to use *H* as a size parameter instead of *R,* even if the former does not explicitly appear in the equation of motion.

Fig. 8 (a-c) offers the displacement of a rocking oscillator as function of its slenderness α, and for 2*H=2, 4, 10, 20, 80,* and *1000m*, for a selection of the FEMA P695 ground motions. The 2*H*=1000m is offered only for reasons of mathematical completeness, to study the limit case of $H \to \infty$. For reasons of plot clarity, each line is plotted only for $\alpha > \alpha_{\text{crit}}$, where α_{crit} is the minimum slenderness angle for which the block overturns. We observe that all blocks of same slenderness angle present roughly the same displacement, as long as they are not close to overturning. The same observation holds for all the ground motions of FEMA P695.

As analysis and design of a rocking structure would not involve a single ground motion, but a set of design motions, it makes sense to study the problem by applying sets of multiple excitations and comparing the statistics of the results [10] (e.g. the median displacement among all the ground motions of the excitation set). To this end, this paper examines the spectra of the median of the displacement for 7 variations of the near-field pulse-like FEMA P695 set: a) Unscaled ground motions, b) scaled so that their PGA is equal to $0.5\overline{PGA}$, or $\overline{PGA}$, or $2\overline{PGA}$, c) scaled so that their PGV is equal to $0.5\overline{PGV}$, or $\overline{PGV}$, or $2\overline{PGV}$, where $\overline{PGA}$, $\overline{PGV}$ are defined as

$$\overline{PGA} = \underset{i=1\ldots N}{median}\left(\sqrt{PGA_{i_x} \times PGA_{i_y}}\right) \tag{16}$$

$$\overline{PGV} = \underset{i=1\ldots N}{median}\left(\sqrt{PGV_{i_x} \times PGV_{i_y}}\right) \tag{17}$$

where *N* is the number of the ground motions and *x* and *y* are the two components of each ground motion. Note that each horizontal component of each ground motion is treated as an independent motion. Fig. 8 (d-i) plots the spectra for some of the above cases: Ground motions scaled so that their PGA is equal to $\overline{PGA}$ (d-f) and scaled so that their PGV is equal to $\overline{PGV}$ (g-i). The rest of the scaling combinations can be found in [50].

The following observations can be made:

a) The median spectra are smoother, likewise design elastic spectra that were derived by statistical processing of elastic spectra of single ground motions are smoother than single ground motion spectra

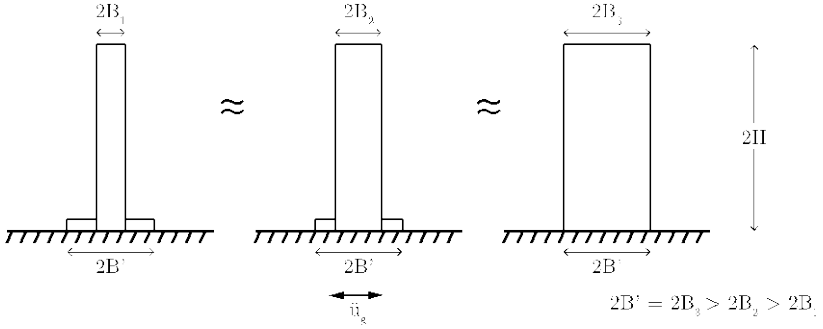

Fig. 7 – Rocking oscillators of equal height

b) As long as the system is not close to overturning, the displacement does not depend on the size of the block. For this part of the spectrum, instead of computing a different spectrum for each block size, one can compute the design spectrum for $2H \to \infty$ ($2H$ = 1000m seems an adequate value) and use it to calculate the displacement *demand* on any rocking structure (i.e. $u_{max}=f(\alpha)$). We name the above finding "equal displacement rule" for rocking structures.

c) As the system gets closer to overturning the equal displacement rule does not apply: smaller systems present larger displacements than larger ones. Moreover, as the system approaches overturning, the slope of the spectrum increases dramatically i.e. a small decrease in tanα leads to very large increase in displacement. This trend dictates that a rational design of a rocking structure would require that this steep part of the spectrum be avoided, because an earthquake slightly stronger than the design one would cause a tremendous increase in displacement. Therefore, the equal displacement rule applies to the rational design region.

d) The form of the spectrum for all 3 sets of ground motions presents some repetitive pattern:
   i. As α tends to zero, u_{max} tends to a finite value. For spectra of individual ground motions, this value is $\frac{3}{2}PGD$.
   ii. As α increases from zero, the displacement demand amplifies 2-2.5 times and reaches a plateau.
   iii. Further increase of α leads to a monotonic decrease of the displacement demand.
   iv. Naturally, when tanα reaches PGA/g, the displacement demand becomes zero, as there is no uplift.

4.3 Preliminary design based on the equal displacement rule

If not for a final design, the equal displacement rule can be used for preliminary calculations. Indeed, it is not an exact method, but a preliminary design method that does not aim at being exact, but at providing a tool for initial calculations, that for certain cases and required degree of accuracy can be enough. The same holds for yielding structures, where the "equal displacement rule" is used for many structural systems, while for more complicated systems it is used only for preliminary design and then more refined methods are applied. It could be stated that the findings of this paper constitute the generalization of equal displacement rule from yielding to rocking systems. This section proposes a methodology to design a rocking structure based on the equal displacement rule:

a) On the u_{max} – tanα curve, we plot the capacity line $u_C = 2H\tan\alpha$.

b) We determine the intersection of the capacity line and the 2H = ∞ line. We define the abscissa of this point as $\tan\alpha_k$.

c) We use a multiplier of 2.5 to determine the design slenderness: $\tan\alpha_D = 2.5\tan\alpha_k$. The multiplier serves as a safety factor to move the design point away from the steep part of the spectrum.

Fig. 9 outlines the design procedure applied for a rocking bridge with columns of 6.7m height ($2H$ = 6.7m). Based on Makris and Vassiliou [13] the response of the frame is equal to the response of a solitary block of $2H$ = 10m. For this bridge, 21 design scenarios are explored, corresponding to the different scaling of the ground motions described in section 4.2. Fig. 10 summarizes the findings for the 21 design scenarios and compare the displacement predicted by the demand spectrum ($2H$ = 1000m) to the displacement predicted by the $2H$=10m spectrum. We observe that in all but two cases (near fault pulse-like scaled to $0.5\overline{PGA}$ and near fault non-pulse-like scaled to $2\overline{PGA}$) the error in predicting the median displacement is less than 20%. In all cases, the error is smaller than 40%, and no system overturned.

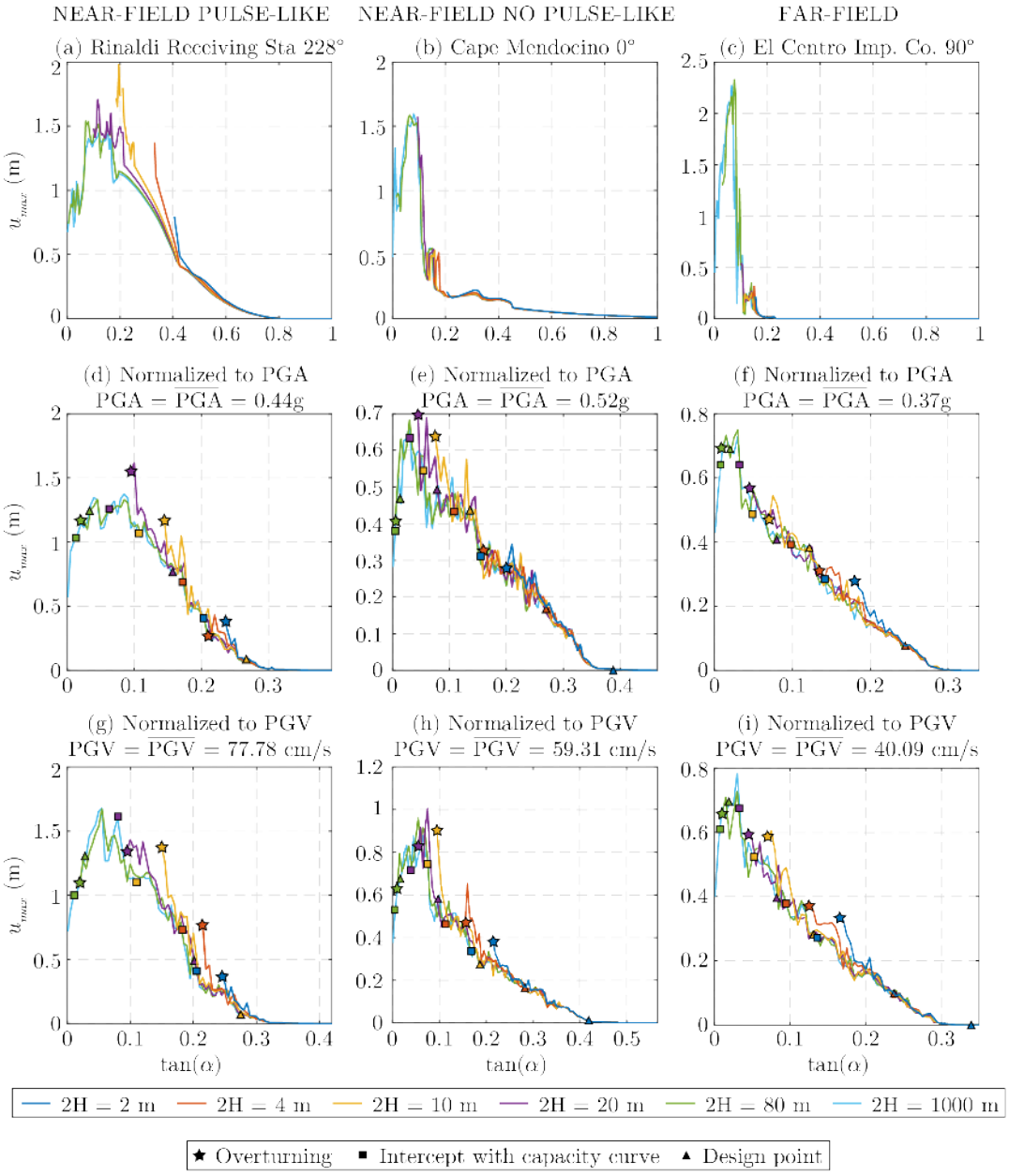

Fig. 8 – Displacement of a rocking oscillator as function of its slenderness *α (a-c);* Median Displacement Spectra (*d-i*)

5. Conclusions

The widely used description of the rocking block via its rotation is correct, but not optimal. It reveals that larger blocks are more stable and that higher frequency pulses present less overturning potential. However, it does not reveal the "equal displacement rule of rocking structures", namely that a large and a small block of the same aspect ratio will present the same top displacement, if they both are not close to overturning. Not being close to overturning is a design necessity anyway, therefore, for the scope of design, we can claim that the displacement demand is the same and it only depends on the slenderness, not on the size of the block. The above is illustrated for both analytical pulse excitations and for sets of recorded ground motions. Based on the above, a design method that uses a size-independent rocking spectrum is suggested. This should be taken into account when intensity measures for rocking structures [55-58] designed not to get close to overturning are explored.

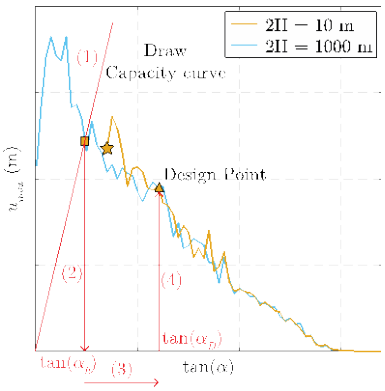

Fig. 9 – Design procedure

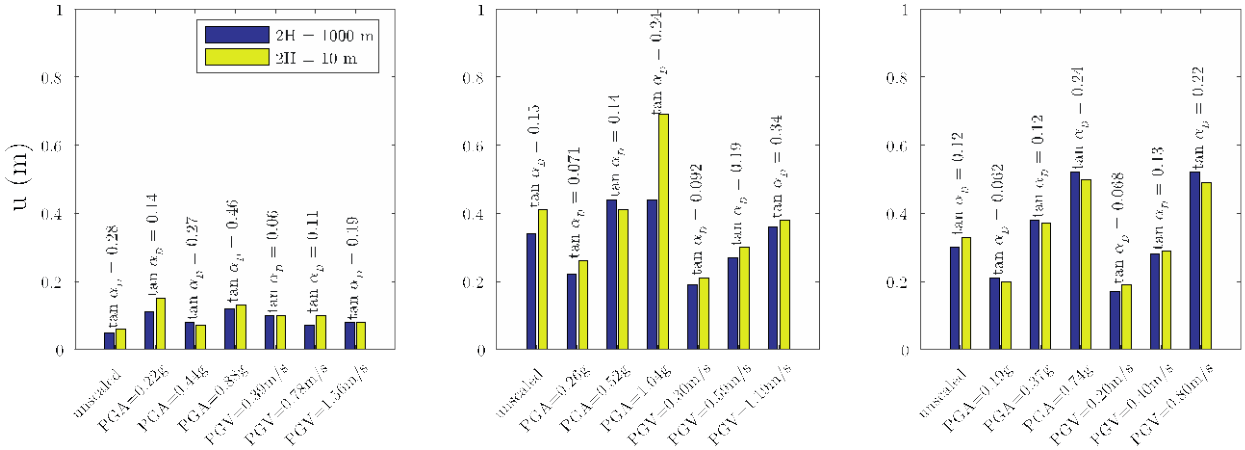

Fig. 10 – Comparison of the displacement response at the design point. Predictions based on the 2*H*=1000m and on the 2*H*=10m spectra.

6. Acknowledgments

This work was supported by the ETH Zurich under Grant ETH-10 18-1. The methods, results, opinions, findings and conclusions presented in this report are those of the authors and do not necessarily reflect the views of the funding agency.

6. References

[1] Housner GW (1963): The behavior of inverted pendulum structures during earthquakes. *Bulletin of the seismological society of America*, **53** (2), 403-417.

[2] DeJong MJ, Dimitrakopoulos, EG (2014): Dynamically equivalent rocking structures. *Earthquake Engineering & Structural Dynamics*, **43** (10), 1543-1563.

[3] Di Egidio A, Alaggio R, Contento A, Tursini M, Della Loggia E (2015): Experimental characterization of the overturning of three-dimensional square based rigid block. *International Journal of Non-Linear Mechanics*, **69**, 137-145.

[4] Vassiliou MF, Truniger R, Stojadinović B (2015): An analytical model of a deformable cantilever structure rocking on a rigid surface: development and verification. *Earthquake Engineering & Structural Dynamics*, **44** (15), 2775-2794.

[5] Truniger R, Vassiliou MF, Stojadinović B (2015): An analytical model of a deformable cantilever structure rocking on a rigid surface: experimental validation. *Earthquake Engineering & Structural Dynamics*, **44** (15), 2795-2815.

[6] Dimitrakopoulos EG, Fung EDW (2016): Closed-form rocking overturning conditions for a family of pulse ground motions. *Proceedings of the Royal Society A*, **472** (2196), 20160662.

[7] Makris N, Kampas G (2016): Size versus slenderness: two competing parameters in the seismic stability of free-standing rocking columns. *Bulletin of the Seismological Society of America*, **106** (1), 104-122.
[8] Giouvanidis AI, Dimitrakopoulos EG (2017): Nonsmooth dynamic analysis of sticking impacts in rocking structures. *Bulletin of Earthquake Engineering*, **15** (5), 2273-2304.
[9] Thiers-Moggia R, Málaga-Chuquitaype C (2019): Seismic protection of rocking structures with inerters. *Earthquake Engineering & Structural Dynamics*, **48**, 528-547.
[10] Bachmann JA, Strand M, Vassiliou MF, Broccardo M, Stojadinović B (2018): Is rocking motion predictable?. *Earthquake Engineering & Structural Dynamics*, **47** (2), 535-552.
[11] Kalliontzis D, Sritharan S (2018): Characterizing Dynamic Decay of Motion of Free-Standing Rocking Members. *Earthquake Spectra*, **34** (2), 843-866.
[12] Avgenakis E, Psycharis IN (2019): Determination of the nonlinear displacement distribution of the semi-infinite strip–Application to deformable rocking bodies. *International Journal of Solids and Structures*, **170**, 22-37.
[13] Makris N, Vassiliou MF (2013): Planar rocking response and stability analysis of an array of free standing columns capped with a freely supported rigid beam, *Earthquake Engineering & Structural Dynamics*, **42** (3), 431-449.
[14] Makris N, Vassiliou MF (2014): Are Some Top-Heavy Structures More Stable?. *Journal of Structural Engineering,* **140** (5), 06014001.
[15] Makris N, Vassiliou MF (2014): Dynamics of the rocking frame with vertical restrainers. *Journal of Structural Engineering*, **141** (10), 04014245.
[16] Dimitrakopoulos EG, Giouvanidis AI (2015): Seismic Response Analysis of the Planar Rocking Frame. *Journal of Engineering Mechanics*, **141** (7), 04015003.
[17] Vassiliou MF, Makris N (2015): Dynamics of the Vertically Restrained Rocking Column. *Journal of Engineering Mechanics*, **141** (12), 04015049.
[18] Giouvanidis AI, Dimitrakopoulos EG (2017): Seismic performance of rocking frames with flag-shaped hysteretic behavior. *Journal of Engineering Mechanics*, **143** (5), 04017008.
[19] Agalianos A, Psychari A, Vassiliou MF, Stojadinovic B, Anastasopoulos I (2017): Comparative Assessment of Two Rocking Isolation Techniques for a Motorway Overpass Bridge. *Frontiers in Built Environment*, **3**, 47.
[20] Vassiliou MF, Mackie KR, Stojadinović B (2017): A finite element model for seismic response analysis of deformable rocking frames. *Earthquake Engineering & Structural Dynamics*, **46**, 447–466.
[21] Vassiliou MF, Burger S, Egger M, Bachmann JA, Broccardo M, Stojadinovic B (2017): The three-dimensional behavior of inverted pendulum cylindrical structures during earthquakes. *Earthquake Engineering & Structural Dynamics*, **46** (14), 2261-2280.
[22] Vassiliou MF (2018): Seismic response of a wobbling 3D frame. *Earthquake Engineering & Structural Dynamics*, **47** (5), 1212-1228.
[23] Thomaidis IM, Kappos AJ, Camara A (2019): Dynamics and seismic stability of planar symmetric rocking bridges. *2nd International Conference on Natural Hazards and Infrastructure,* Chania, Greece.
[24] Xie Y, Zhang J, DesRoches R, Padgett JE (2019): Seismic fragilities of single-column highway bridges with rocking column-footing. *Earthquake Engineering & Structural Dynamics*, **48** (7), 843-864.
[25] Bachmann JA, Vassiliou MF, Stojadinovic B (2019): Rolling and rocking of rigid uplifting structures. *Earthquake Engineering & Structural Dynamics*, **48** (14), 1556-1574.
[26] Bachmann JA, Vassiliou MF, Stojadinović B (2018): Dynamics of rocking podium structures. *Earthquake Engineering & Structural Dynamics*, **46** (14), 2499-2517.
[27] Aghagholizadeh M, Makris N (2018): Earthquake response analysis of yielding structures coupled with vertically restrained rocking walls. *Earthquake Engineering & Structural Dynamics*, **47** (15), 2965-2984.
[28] Ríos-García G, Benavent-Climent A (2020): New rocking column with control of negative stiffness displacement range and its application to RC frames. *Engineering Structures*, **206**, 110133.
[29] Konstantinidis D, Makris N (2010): Experimental and analytical studies on the response of 1/4-scale models of freestanding laboratory equipment subjected to strong earthquake shaking. *Bulletin of earthquake engineering*, **8** (6), 1457-1477.
[30] Wittich CE, Hutchinson TC (2015): Shake table tests of stiff, unattached, asymmetric structures. *Earthquake Engineering & Structural Dynamics*, **44** (14), 2425-2443.
[31] Dar A, Konstantinidis D, El-Dakhakhni WW (2016): Evaluation of ASCE 43-05 seismic design criteria for rocking objects in nuclear facilities. *Journal of Structural Engineering*, **142** (11), 04016110.
[32] Sextos AG, Manolis GD, Ioannidis N, Athanasiou A (2017): Seismically induced uplift effects on nuclear power plants. Part 2: Demand on internal equipment. *Nuclear Engineering and Design*, **318**, 288-296.
[33] Dar A, Konstantinidis D, El-Dakhakhni W (2018): Seismic response of rocking frames with top support eccentricity. *Earthquake Engineering & Structural Dynamics*, **47** (12), 2496-2518.

[34] Voyagaki E, Kloukinas P, Dietz M, Dihoru L, Horseman T, Oddbjornsson O, Crewe AJ, Taylor CA, Steer A (2018): Earthquake response of a multiblock nuclear reactor graphite core: Experimental model vs simulations. *Earthquake Engineering & Structural Dynamics*, **47** (13), 2601-2626.
[35] Di Sarno L, Magliulo G, D'Angela D, Cosenza E (2019): Experimental assessment of the seismic performance of hospital cabinets using shake table testing. *Earthquake Engineering & Structural Dynamics*, **48** (1), 103-123.
[36] Mouzakis HP, Psycharis IN, Papastamatiou DY, Carydis PG, Papantonopoulos C, Zambas C (2002): Experimental investigation of the earthquake response of a model of a marble classical column. *Earthquake Engineering & Structural Dynamics*, **31** (9), 1681-1698.
[37] Papantonopoulos C, Psycharis IN, Papastamatiou DY, Lemos JV, Mouzakis HP (2002): Numerical prediction of the earthquake response of classical columns using the distinct element method. *Earthquake Engineering & Structural Dynamics*, **31** (9), 1699-1717.
[38] Papaloizou L, Komodromos P (2009): Planar investigation of the seismic response of ancient columns and colonnades with epistyles using a custom-made software. *Soil Dynamics and Earthquake Engineering*, **29** (11), 1437-1454.
[39] Vassiliou MF, Makris N (2012): Analysis of the rocking response of rigid blocks standing free on a seismically isolated base. *Earthquake Engineering & Structural Dynamics*, **41** (2), 177-196.
[40] Stefanou I, Psycharis I, Georgopoulos, IO (2011): Dynamic response of reinforced masonry columns in classical monuments. *Construction and Building Materials*, **25** (12), 4325-4337.
[41] Tondelli M, Beyer K, DeJong M (2016): Influence of boundary conditions on the out-of-plane response of brick masonry walls in buildings with RC slabs. *Earthquake Engineering & Structural Dynamics*, **45** (8), 1337-1356.
[42] Casapulla C, Giresini L, Lourenço, PB (2017): Rocking and Kinematic Approaches for Rigid Block Analysis of Masonry Walls: State of the Art and Recent Developments. *Buildings*, **7** (3), 69.
[43] Kalliontzis D, Schultz AE (2017): Characterizing the In-Plane Rocking Response of Masonry Walls with Unbonded Posttensioning. *Journal of Structural Engineering*, **143** (9), 04017110.
[44] Mehrotra A, DeJong MJ (2018): The influence of interface geometry, stiffness, and crushing on the dynamic response of masonry collapse mechanisms. *Earthquake Engineering & Structural Dynamics*, **47** (13), 2661-2681.
[45] Giresini L, Sassu M, Sorrentino L (2018): In situ free-vibration tests on unrestrained and restrained rocking masonry walls. *Earthquake Engineering & Structural Dynamics*, **47** (15), 3006-3025.
[46] Giordano N, De Luca F, Sextos A (2020): Out-of-plane closed-form solution for the seismic assessment of unreinforced masonry schools in Nepal. *Engineering Structures*, **203**, 109548.
[47] Zhang J, Makris N (2001): Rocking response of free-standing blocks under cycloidal pulses. *Journal of Engineering Mechanics*, **127** (5), 473-483.
[48] Buckingham E (1914): On physically similar systems; illustrations of the use of dimensional equations. *Physical Review*, **4** (4), 345–376.
[49] Dimitrakopoulos EG, DeJong MJ (2012): Revisiting the rocking block: closed-form solutions and similarity laws. *Proceedings of the Royal Society A*, **468** (2144), 2294-2318
[50] Reggiani Manzo N, Vassiliou, MF (2019): Displacement-based analysis and design of rocking structures. *Earthquake Engineering & Structural Dynamics*, **48** (14), 1613-1629.
[51] Barenblatt GI (1996): *Scaling, self-similarity, and intermediate asymptotics: dimensional analysis and intermediate asymptotics*, Cambridge University Press, Vol. 14.
[52] Blöchlinger (2016): *Rigid body rocking spectra for recorded earthquake ground motions*, Master's Thesis, ETH Zurich.
[53] FEMA P695. Quantification of Building Seismic Performance Factors. Washington, D.C: Rep. FEMA P695, Federal Emergency Management Agency; 2009.
[54] Vassiliou MF, Mackie KR, Stojadinović B (2014): Dynamic response analysis of solitary flexible rocking bodies: modeling and behavior under pulse-like ground excitation. *Earthquake Engineering & Structural Dynamics,* **43**, 1463–1481.
[55] Dimitrakopoulos EG, Paraskeva TS (2015): Dimensionless fragility curves for rocking response to near-fault excitations. *Earthquake Engineering & Structural Dynamics*, **44** (12), 2015-2033.
[56] Pappas A, Sextos A, Da Porto F, Modena, C (2017): Efficiency of alternative intensity measures for the seismic assessment of monolithic free-standing columns. *Bulletin of Earthquake Engineering*, **15** (4), 1635-1659.
[57] Giouvanidis AI, Dimitrakopoulos EG (2018): Rocking amplification and strong-motion duration. *Earthquake Engineering & Structural Dynamics*, **47** (10), 2094-2116.
[58] Kavvadias IE, Papachatzakis GA, Bantilas KE, Vasiliadis LK, Elenas A (2017): Rocking spectrum intensity measures for seismic assessment of rocking rigid blocks. *Soil Dynamics and Earthquake Engineering*, **101**, 116-124.